Predicting the outcome of a PCR test for COVID-19 using a routine blood exam: A replication

An example of how AI can help identify possible infections in a primary care/triage system

By

Lukas Schießer

Thesis Supervisor:
Johannes Schrumpf M. Sc., Institute of Cognitive Science, Osnabrück University
Thesis Supervisor:
Dr. Tobias Thelen, Institute of Cognitive Science, Osnabrück University

Abstract

This thesis replicates a study training different classifiers to predict the outcome of a PCR test for COVID-19 based on a routine blood exam. This thesis reproduces the Random Forest and Logistic Regression classifiers. They were trained using 5-fold nested cross validation and compared to the classifiers' performance in the original paper. The replicated classifiers underperformed when contrasted with the original classifiers. However, they were still statistically significant and showed congruency with regards to findings from medical research. Models like these can help assist medical staff during situations where testing capacities are restricted due to shortages in material or personnel by focusing testing efforts on patients with a high probability of having contracted the virus.

Acknowledgements

I want to thank...

Contents

List of Figures

List of Tables

Chapter 1

Introduction

In December 2019, a novel coronavirus named Sars-CoV-2 emerged in Wuhan China. It spread rapidly around the world, leading the World Health Organization (WHO) to declare a global pandemic in March 2020. To date, more than one year post-outbreak, the coronavirus disease COVID-19 caused by the Sars-CoV-2 coronavirus has infected more than 100 million people and has claimed more than 2 million dead [19]. Due to its unprecedented nature and its high ability to spread in the general population, it is crucial to identify infectious people early and isolate them as soon as possible in order to prevent the spread of the virus. Especially the high proportion of asymptomatic but infectious patients is a major challenge for the containment of this pandemic [30]. The main method to identify the virus is the reverse polymerase chain reaction (PCR) or reverse transcriptase-PCR (RT-PCR) technique. It identifies the virus by detecting the presence of its genetic material in a sample. Unfortunately, the execution of the test is very time-consuming and takes at least four to five hours under optimal condition. Furthermore, the execution requires the use of special equipment and reagents, the involvement of skilled and qualified staff, personnel to collect samples, and relies on the proper genetic conservation of the RNA sequences [41, 16]. Medical staff in emergency departments have to assess the probability of a Sars-CoV-2 infection for each patient during triage. In the event of a shortage of testing capabilities, this can be particularly difficult to do. Algorithmic solutions could provide assistance and reduce the uncertainty in who should be tested for the disease. There are different approaches for this algorithmic solution. One approach is based on computer tomography scans or chest X-rays [45]. Models based on chest X-rays are often associated with high rates of false negative predictions [45, 43]. Whereas models based on CT scans are not advantageous in comparison with a PCR test as they share common requirements like specialized

equipment, long duration and high costs. Another approach is the use of blood test which are generally available, deliver results much faster taking only a minimum of 15 minutes in an emergency setting and are much more cost effective. This thesis replicates a feasibility study implementing different classifiers to predict the outcome of a PCR test for COVID-19 based on a routine blood exam.

Chapter 2

Materials and Methods

2.1 Data

The data used to train the classifiers was provided by Brinati et al. [6]. It was collected between the end of February 2020 and mid of March 2020 from patients admitted to the *IRCSS Ospedale San Raffaele* in Milan, Italy and consists of 279 individuals who were selected randomly. For each individual, the data set provides their age, gender, the results of a routine blood screening, and a PCR test for Sars-CoV-2. A complete overview of the recorded variables is provided in Table A.1. The target variable *Swab* is binary and indicates the result of a PCR-test for Sars-CoV-2 taken by a nasopharyngeal swab. 0 indicates a negative test, while 1 indicates a positive test. The data set is slightly imbalanced towards positive cases, with 102 (37%) negative cases and 177 (63%) positive cases.

The data was cleaned and wrangled in order to properly analyze it. Since the variable *Gender* was provided as a string, it was transformed into two binary numerical variables called *female* and *male* by one-hot encoding. Further, two values of the variable *Age* were replaced with a missing value indicator, specifically the values 0 and 1. This was sensible, seeing that there was no other data recorded from minors. Thus these two values can be presumed to be input errors during the collection process. Further, the variable *Lymphocytes* had to be recasted to a numeric format because there was an input error for one of its values rendering the column's contents a string instead of a numerical value. This process created one missing value in place of the erroneous value.

Table A.4 provides standard statistics for the numerical features of the data set, specifically their measurement unit, mean, standard deviation and median. These standard statistics in combination with the kernel density plots provided in Figure

B.1 show that all features are skewed relative to a (standard) normal distribution. Blood values are skewed positively, exhibiting a right-tailed distribution because, for most blood values, a lower or centered value is a sign of better health. Age is skewed negatively, exhibiting a left-tailed distribution since COVID-19 affected older individuals more severely than younger individuals, especially in Italy [33].

In order to confirm the observation of non-normality, a Shapiro-Wilk test for normality was performed. The test probes the null-hypothesis that the samples of a variable come from a normally distributed population. If the test's p-value is smaller than 0.05, a commonly chosen α level, the null-hypothesis is rejected, meaning the data is not normally distributed [39]. The test results are provided in Table A.5 and show that all of the variables are non-normally distributed.

Table A.3 shows that most features have missing values. 196 samples have at least one feature missing, which amounts to 70% of the data. Due to the small data set size, it is not feasible to exclude these individuals from the analysis process. It is rather more constructive to use an imputation method that models the missing values based on the data set's observed values. Therefore, Brinati et al. chose to use *Multivariate Imputation by Chained Equations*.

2.2 Multivariate Imputation by Chained Equations

Multivariate Imputation by Chained Equations or *MICE* for short is an imputation method proposed by Buuren and Groothuis-Oudshoorn [8]; it is also known as *fully conditional specification* (FCS). MICE is a method that imputes missing data by estimating a set of possible values from distributions of observed data. Each variable with missing data x_n is regressed on all other variables $x_1, ..., x_n$ which are restricted to the occurrences with observed data in x_k. MICE assumes that the data are missing at random (MAR). That is, the probability of missing data does not depend on the unobserved data but is only dependent (conditional) on the observed data. Due to its individualistic approach, MICE can handle variables of different types using different modeling choices for different variable types.

The imputation process is based on the following four main steps [44, 4]: Firstly, all missing values are imputed using a simple imputation method (e.g., mean imputation). These imputations can be thought of as "place holders" used during the first modeling phase. During step 2, the "place holder" imputations for one variable x are set back to missing. In step 3, all observed values from variable x in step 2 are regressed on the imputations model's other variables. Since this is the model

building phase, this step only uses samples where x has observed values. Therefore, x is the dependent variable, and all other variables are independent variables used in the regression model. In step 4, the missing values in x are replaced with imputations (predictions) from the regression model built in step 3. All values of x, the observed and the imputed values, are then used in subsequent regression models of other variables.

Steps 2-4 are repeated for every variable with missing data. After the algorithm cycled through all variables, one iteration is completed. Steps 2-4 are repeated for a user-specified number of cycles. Generally, ten to twenty cycles should suffice to stabilize the imputation results, indicating that the parameters controlling the imputations should have converged by then. This imputation process is usually repeated m times, creating m slightly differently imputed data sets, which are then used in the subsequent analysis. According to [7, 4, 44], already a small number of imputed data sets, usually three to ten, is sufficient to provide sensible results during analysis. It can, of course, be advantageous to use a higher number of imputed data sets to get a broader range of estimates. However, setting m higher requires more computations and storage and may not be worth preoccupying these extra resources [7].

2.3 Classifiers

The original paper implements eight classifiers, namely Random Forest, Logistic Regression, Decision Tree, K-nearest Neighbors, Naive Bayes, Support Vector Machines, Extremely Randomized Trees, and three-way Random Forest [6]. Here, I will reproduce the Random Forest, Logistic Regression, and Decision Tree classifiers. The following section introduces them.

2.3.1 Decision Tree

Since Decision Trees are the basic building block of Random Forest and we will use them during the validation it is necessary to take a closer look at them [5]. Thereby the use of Random Forests will be motivated and we will gain some insights into the workings of the Random Forest Classifier. A Decision Tree has a flowchart-like structure where each internal or decision node tests an attribute. Each branch corresponds to one attribute value, and each leaf node represents a classification. It is built up using the ID3 algorithm [36].

ID3 tries to determine the best attribute of a given data set by the distribution of its values. The best attribute is then used as a root of the Decision Tree, and a branch is created for every value this attribute can take, which also creates a subset of the data set that only has the attribute value of the branch. This process is repeated for every branch with the remaining subset of the training set until a leaf node is reached. [34]

ID3 can use many different measures to decide which is the best attribute. Two of the most popular ones are Information Gain and the Gini Impurity.

Information Gain uses the entropy measure to compute the impurity also known as heterogeneity of an attribute. Entropy originates from information theory and describes the average information content of an attribute's possible outcome, it is calculated, as shown in Equation 2.1 where S is a set of samples and C are the possible outcome labels of the target variable. A high entropy represents a high average information content in an attribute [24]. Information Gain measures the expected reduction in entropy of a set S caused by learning the state of a random attribute A. It is calculated, as shown in Equation 2.2, and can be described as the difference between the entropy of a set S and the weighted average of the child entropies $E(S_v)$ where S_v is a subset of S where the attribute A has the value v. This is computed for all remaining attributes, the attribute that maximizes the differences is then selected as a new node [34].

$$E(S) = \sum_{i=1}^{C} -p(i)\ log_2(p(i)) \tag{2.1}$$

$$Gain(S, A) = E(S) - \sum_{v}^{V} \frac{|S_v|}{S} E(S_v) \tag{2.2}$$

The Gini Impurity or Gini index measures the impurity in a set S that is the probability of incorrect classification of a random sample. It is calculated as shown in Equation 2.3. The measure on which the algorithm bases its decision which attribute to select as a node is called the Gini gain. It is calculated as shown in Equation 2.4 and can be described as the average Gini Impurity. The attribute with the lowest value is selected for the Gini gain since we want to minimize the attributes' incorrect classification [36].

$$G = 1 - \sum_{i=1}^{C} p(i)^2 \tag{2.3}$$

$$Gini(S, A) = \sum_{i=1}^{C} \frac{|S_i|}{|S|} G(S_i) \tag{2.4}$$

2.3.2 Random Forest

The Random Forest Classifier is an ensemble classifier that uses multiple Decision Tree instances to classify the given data. It uses two methods to diversify the different classifications of the Decision Tree instances called tree bagging and feature bagging [5].

During tree bagging, the Decision Tree is not trained on the whole training set but a subset of the training set. The subsets are generated by sampling the original data set with replacement. A certain percentage of samples is selected from the original data set and the remaining percentage are duplicates of the already selected samples. This process generates new bagged training sets S_i with the same size as the original training set S. If the size of the bagged set is smaller than the size of the original set, this process is called sub-bagging [5, 38].

Feature bagging or feature subset selection limits the number of features the individual Decision Trees can use at each new split in consideration. For each decision node consideration, several features are randomly selected and presented to the Decision Tree algorithm. A hyperparameter controls the number of features available to the algorithm. For classification problems, this is usually set to $\sqrt{p}$ where p is the number of features present in the complete data set [5, 3].

Each Decision Tree in the forest generates a classification. A majority vote over all Decision Trees determines the final classification of the Random Forest. Using tree and feature bagging, Random Forests average over all individual Decision Tree models, reducing the variance of classification and avoiding overfitting [3].

2.3.3 Logistic Regression

Logistic Regression is a modification of linear regression that models the probability $p(X)$ that a sample X has the label 1. To do so, it uses a special form of the sigmoid function called the logistic function where $\mathbf{X}$ is a vector or matrix of samples and $\vec{\beta}$ is a vector of the coefficients [38, 3]:

$$p(\mathbf{X}) = \phi_{sig}(\mathbf{X}) = \frac{e^{\mathbf{X}\vec{\beta}}}{1 + e^{\mathbf{X}\vec{\beta}}} = \frac{1}{1 + e^{-\mathbf{X}\vec{\beta}}} \tag{2.5}$$

After some manipulation, we can see

$$\frac{p(\mathbf{X})}{1 - p(\mathbf{X})} = e^{\mathbf{X}\vec{\beta}} \qquad (2.6)$$

The left-hand side of Equation 2.6 is called odds. It can take a value between 0 and ∞ indicating very low or very high probabilities of having the label 1. After applying the logarithm to both sides of Equation 2.6, the log-odds or logit is obtained (Equation 2.7), which is linear in X [28, 3].

$$ln\Big(\frac{p(\mathbf{X})}{1 - p(\mathbf{X})}\Big) = \mathbf{X}\vec{\beta} \qquad (2.7)$$

Since β_0 and all β_i of the vector $\vec{\beta}$ are unknown, they must be estimated on the available training data. The method that is used to achieve this is called maximum likelihood estimation (MLE). MLE tries to find estimates for the coefficients β such that the estimated probability $\hat{p}(x_i)$ of having label 1 for each individual is as close as possible to the individual's observed label. In other words, MLE tries to find estimates for the coefficients β of the model $P(\mathbf{X})$ described in Equation 2.5 such that the resulting probability is close to one if the individual's observed label is 1 and close to zero if the individual's label is 0. This can be formalized as a likelihood function as shown in Equation 2.8. The estimates for β are then chosen to maximize the likelihood function [3].

$$L(\vec{\beta}|\vec{y}, \mathbf{X}) = \prod_i p(x_i)^{y_i}(1 - p(x_i))^{(1-y_i)} \qquad (2.8)$$

2.4   Model Training

Random Forest and Decision Tree are trained using 5-fold nested cross validation. In each outer fold of the nested cross validation, the data is imputed using MICE and then split into training and test data. Since MICE usually generates several imputed data sets to account for the uncertainty in the imputation process, there are 5 different models for each classifier per fold. The cross validation's inner fold is used to determine the best hyperparameter combination for the classifiers using *Grid Search*, also called hyperparameter tuning [32]. Figure B.2 explains this process in further detail. The parameters for Random Forest are:

- Number of trees in the forest: [10, 100, 500]

- Number of features to consider looking for the best split: [4, 8, 12, 16]

- Quality of split measure: Gini Impurity or Information Gain

For Logistic Regression, Grid Search seeks for an optimum among the following hyperparameters:

- Inverse of regularization strength C: [0.001, 0.01, 0.1, 1, 10, 100, 1000]

- Penalty: L1 or L2 regularization

- Algorithm to use during optimization problem: liblinear or saga

- Maximal iteration: [200, 300, 400, 500]

The remaining hyperparameters use the default values specified in the documentation of sklearn for Random Forests and Logistic Regression [32]. Grid Search selects the best hyperparameters according to the highest accuracy value.

After the training, the models are evaluated using accuracy, balanced accuracy, sensitivity, specificity, positive predictive value, and area under the ROC curve which are explained in the next section. The hyperparameters of the best performing models for Random Forest and Logistic Regression are then used to obtain the final classifiers. For the validation, the whole data set is split into training and validation data according to an 80:20 ratio. The data set is imputed before the split due to how the `mice()` package runs in R. The classifiers are trained on the training data and then validated using the validation data. In addition to the evaluation metrics above, the final classifiers were also evaluated using the ROC curve and the precision-recall curve. Additionally, the precision-recall curve is used to assess the classifiers' performance regarding the slight imbalance in the data set. To further gain some insights into the Random Forest's classification reasoning, a Decision Tree is trained using the standard hyperparameters according to the sklearn implementation [32].

To implement this procedure, the Python libraries scikit-learn, pandas, and numpy are used. To implement the imputation method, the R library `mice()` is used and connected to the Python implementation using a bridge package called rpy2. The R implementation of the imputation method is used instead of a Python implementation since it provides more functions to inspect the MICE procedure and since it is able to handle non-normally distributed data. To visualize the results, the libraries seaborn and matplotlib are used.

2.5 Evaluation Metrics

The following terms will be used in the equations to describe the evaluation metrics: True Positive, False Positive, False Negative, and True Negative. They are further characterized in Table 2.1.

		True condition	
		Condition positive	Condition negative
Predicted condition	Condition predicted positive	True Positive (TP)	False Positive (FP)
	Condition predicted negative	False Negative (FN)	True Negative (TN)

Table 2.1: Confusion matrix for binary classification

Accuracy describes the closeness of a predicted label to its true label. It is calculated as shown in Equation 2.9. Accuracy alone is not a sensible measure to determine the goodness of fit for a model since the model can be affected by imbalanced data or poor parameter initialization. Accordingly, other measures should be considered during model selection [24].

$$accuracy = \frac{TP + TN}{TP + FP + FN + TN} \tag{2.9}$$

Balanced accuracy is used in addition to the average accuracy due to the slight imbalance in the data set. If the balanced accuracy differs significantly from the average accuracy, the imbalance affects the classifier regarding class prevalence. The balanced accuracy is defined as the average of sensitivity and specificity [24, 6].

$$balanced\ accuracy = \frac{\frac{TP}{TP+FN} \frac{TN}{TN+FP}}{2} \tag{2.10}$$

Sensitivity is interpreted as the proportion of people infected with a disease who will test positive for this disease. It is calculated as shown in Equation 2.11. Since it is only calculated using the part of the population with the disease, sensitivity can only give evidence about the true positive rate and not the test's false positive rate [1].

$$sensitivity = \frac{TP}{TP + FN} \tag{2.11}$$

Specificity is defined as the proportion of people without the disease that are identified correctly, i.e., who tested negative for the disease. It is calculated as shown in Equation 2.12. Specificity only gives information about the proportion of people

without the disease and a negative test and cannot disclose anything about the false negative rate [1].

$$specificity = \frac{TN}{TN + FP} \tag{2.12}$$

The positive predictive value (PPV) measures the post-test probability of the disease given a positive test. It, therefore, refers to the probability that a subject with a positive test has indeed the disease. It is calculated as shown in Equation 2.13 [1].

$$PPV = \frac{TP}{TP + FP} \tag{2.13}$$

The receiver operating characteristic curve (ROC curve) is a commonly used metric to determine a model's performance describing the trade-off between specificity and sensitivity. It is calculated using the prediction scores of a model that are either discriminant values or posterior probabilities [37]. Most models do not produce a classification label as their output but rather a prediction score that is then thresholded to correspond to one of the target variable levels. The metrics mentioned above are all so called single-thresholded metrics since they are defined only for the classifier's thresholded output [37, 24]. Since ROC uses the prediction scores instead of the thresholded output of a model, it can compute the sensitivity and specificity for every sensible threshold. The resulting values are then plotted with sensitivity or true positive rate as the vertical axis and the false positive rate or 1 - specificity as the horizontal axis. The points are interpolated linearly to create the ROC curve [37]. Usually, a reference line is added to the plot illustrating a model's performance that only makes random predictions. The curve for the trained model is expected to be above the reference line at all times. A model with perfect performance will appear in the top left-hand corner of the ROC space where the sensitivity is one, and the false positive rate is zero [24, 20].

The area under the ROC curve can also be measured and is called either AUC for area under the ROC curve or ROC index. It can give a numeric summary of the ROC curve. It is calculated using the ROC curve's integral which can be easily done using the trapezoidal method since the ROC curve is discrete and stepped. A large AUC value indicates a better model performance. As a rule of thumb, an AUC over 0.7 indicates a strong predictive model, and an AUC below 0.6 indicates a weak model. AUC and ROC both are quite robust against imbalanced data, but other non-single-threshold metrics can be used in this case as well [24, 20].

The Precision-Recall curve (PRC) is another non-single-threshold metric that is especially useful when dealing with an imbalanced data set. It calculates the precision and recall values for each feasible threshold. The resulting values are then plotted with precision, also called positive predictive value, as the vertical axis and

recall, also called sensitivity, as the horizontal axis. The points are interpolated non-linearly to create a curve. In contrast to the ROC curve, which uses a fixed reference line, the PRC's baseline is determined by the ratio of positive (P) and negative (N) samples in the data set and represented as $y = \frac{P}{P+N}$. Each point in the PRC plot corresponds to exactly one point in the ROC plot since one of the measures in the plot is the same. The area under the curve can also be calculated for the precision-recall curve similar to the AUC of the ROC curve and is then denoted by AUC (PRC) or average precision. Similarly, a large value for the AUC (PRC) indicates a strong model, and a lower value indicates a weak model [17, 37].

Chapter 3

Results

3.1 Results of own implementation

Table A.6 and A.7 show the mean and standard deviation for the accuracy and balanced accuracy of the models during nested cross-validation. The authors of the original paper provided a 95% confidence interval for these two measures. Since there is no information on how they computed this interval, it is assumed that they used a two-sided Student's t-distribution which is used to estimate the mean of normally distributed populations where sample size is small. It is calculated using the following formula $\bar{x} \pm \frac{t_{\alpha,v}s}{\sqrt{n}}$ where $t_{\alpha,v}$ is the t-value which can be taken from a table with α as the degrees of freedom $n-1$ and v as the confidence level, s is the sample variance, $\bar{x}$ is the sample mean, and n is the number of samples [22]. For the Random Forest, the 95% confidence interval of the average accuracy is [0.76, 0.80] and of the average balanced accuracy is [0.73, 0.77]. For Logistic Regression, the confidence interval of the average accuracy is [0.72, 0.77] and of the average balanced accuracy is [0.68, 0,72]. Since the confidence intervals of the accuracy and balanced accuracy for both classifiers overlap or are near each other, it can be assumed that the slight imbalance of the data set had no significant effect on the classifier and that the classifier therefore is not biased against the outcomes of the target variable. All evaluation metrics for each fold and imputed data set are provided in Table A.9.

The best models where selected by searching for the model with the most numbers of highest evaluation measures. The best Random Forest Classifier used maximally 4 features, 500 estimators and Gini impurity, it achieved an accuracy of 87.5% and a sensitivity of 90%. The best Logistic Regression Classifier used a C of 10, a maximal iteration of 200, the 'l2' penalty and the 'liblinear' solver, it achieved an accuracy

of 83.9% and a sensitivity of 85%. These settings were then used to retrain the classifiers and compute the validation metrics.

The Random Forest Classifier is also the best performing classifier after retraining it with the best hyperparameter with an accuracy of 76.8% and a balanced accuracy of 73.7%. The Logistic Regression achieves an accuracy of 73.2% and a balanced accuracy of 69.4%. Accordingly, there is also no significant difference between the accuracy and balanced accuracy for all three classifiers, meaning no classifier is biased. The aforementioned metrics are lower than the evaluation metrics since the data set used to train during the validation phase is different from the one used during the evaluation phase due to the way MICE imputes missing data. All single-threshold metrics are provided in Table A.8. The two multi-threshold metrics, ROC and PRC curve, are shown in Figure B.3. Both plots show that the classifiers perform better than the reference line. The values for the area under the ROC and under the PRC curve suggest that Logistic Regression (AUC: 80.8%, AUC (PRC): 85.5%) performs better than the Random Forest (AUC: 80.5%, AUC (PRC): 82.9%) although all other metrics indicate a better performance for the latter. It should be noted that the difference between the AUC scores for both curves are minimal and are not meaningful enough to declare the Logistic Regression as the better classifier. The more apparent differences in the AUC (PRC) for both classifiers on the other hand could indicate that the Logistic Regression is less affected by the imbalance in the data set than the Random Forest is.

The Decision Tree Classifier exhibits a lower discriminative performance especially when looking at the AUC and AUC (PRC) with 68.5% and 69.8% indicating a rather weak classifier. Additionally, it only achieves an accuracy of 71.4% and a balanced accuracy of 68.5%. Despite these low metrics, the Decision Tree can still be used as an aid to help clinicians make quick decisions and to interpret the result of the Random Forest.

Figure B.4 shows all feature importance plots for the three classifiers. The feature importance for Decision Tree and Random Forest were obtained using the sklearn implementation. The implementation calculates the feature importance by quantifying the mean decrease in impurity. It should be noted that impurity-based feature importance can suffer from favoring features with a high number of unique values as well as making predictions based on statistics derived from the training set. This method is therefore not necessarily informative about whether a feature makes for a good prediction or not.[25] For Logistic Regression, the feature importance is inferred by looking at the coefficients of each feature in the data set. A positive coefficient can be interpreted as contributing to a positive (1) result and a negative coefficient can be interpreted as contributing to a negative (0) result. It is difficult

to compare non tree-based feature importance with tree-based importance because they have different scales and means of calculation.

Both tree-based methods show a similar feature importance plot with AST being the most important feature. The remaining features are differently distributed, but mostly exhibit similar values. Consequently, the Decision Tree and its visualization (Figure B.5) in combination with the feature importance plots for both tree-based classifiers can be used to give some rough insights into the classification procedure of the Random Forest.

3.2   Comparison with original paper

The 95% confidence intervals for the accuracy and balanced accuracy of this replication overlap with the ones from the original paper. The average accuracy for Random Forest in the original is [0.74, 0.80] (replication: [0.76, 0.80]) and [0.70, 0.81] (replication: [0.72, 0.77]) for Logistic Regression. The average balanced accuracy in the original is [0.70, 0.82] (replication: [0.73, 0.77]) for Random Forest and [0.65, 0.74] (replication: [0.68, 0.72]) for Logistic Regression. Since there is no information about individual values during the nested cross validation and it is also not reported how the authors computed the 95% confidence intervals, it can be difficult to compare them. Nevertheless, the overlap of the intervals suggests that the classifiers can be compared to a certain degree. Unfortunately, there is no more information about further evaluation metrics.

The validation metrics of the retrained classifiers show a lower performance than the classifiers in the original paper. The differences between the Random Forest and Logistic Regression are however similar to the ones in the original paper. In this replication, the single-threshold metrics are higher for the Random Forest and the multi-threshold metrics are higher for the Logistic Regression reflecting a behavior similar to that in the original paper. The ROC curve for both classifiers exhibits a similar course as in the original except that the curves in the original rise higher in the beginning due to their higher discriminative power. Seeing that the precision-recall curve only plots the performance of the Random Forest, we can only compare these results. The replication and the original differ greatly in this plot, but still exhibiting a similar course at some points, e.g., the sharp drop between sensitivity = [0.0, 0.2].

Chapter 4

Discussion

4.1 Discussion of Results

Although the classifiers perform worse than the ones in the original paper, most recorded metrics still certify them a good discriminative performance. With a sensitivity of 90% for both models and accuracy values between 73% and 76%, the classifiers can still serve as supplementary decision tools to help physicians make decisions about allocating testing based on their predictions and other indicators. Further, the AUC and AUC (PRC) values which are over 80% for both classifiers indicate that they are indeed strong classifiers. Due to the slight imbalance of the data set, it is favorable to examine the classifiers regarding this potential source of bias. If there was a significant difference between the accuracy and the balanced accuracy for a classifier, it would entail a bias against one of the target outcomes. This is not the case for both classifiers. Moreover, the high values of the AUC (PRC) suggest that the classifiers are not significantly affected by the imbalance of the data. The metrics can also make statements about an infection event and the expressiveness of the classifiers. The high sensitivity signals that 90% of patient who get a positive result actually have the disease. While the specificity is comparatively low, it does not necessarily pose a problem. A low specificity in combination with a high sensitivity indicates a higher false positive rate than a high false negative rate.[1] Therefore, if the result of the classifier is negative, it will be safe to assume that a PCR test for COVID-19 will also be negative and thus the patient will not have the disease. This is more desirable because it is better to be over cautious and recommend more tests.

Since the question about the relevance of the classifier has been clarified, this para-

graph deals with the internal classification reasoning of the classifier and their accordance with findings from medical studies. When inspecting the feature importance plots for the tree-based classifiers, both plots (Figure B.4a and B.4b) show that the AST, WBC, CRP and lymphocyte counts are under the five most important features. In the Random Forest, the LDH count replaces the age variable in Decision Trees. For the Logistic Regression (Figure B.4c), the eosinophil, WBC, basophil and lymphocyte counts are the most important features together with the age variable. All feature importance measures have the WBC and lymphocyte count in common. Multiple studies also show that these two blood values are significant indicators for a COVID-19 infection. The WBC or white blood cell count refers to the actual number of white blood cells per volume of blood while the lymphocytes are a subgroup of white blood cells involved in eliciting a immune response to foreign agents.[13, 35] During an infection with Sars-CoV-2, the WBC and lymphocyte counts will decrease since this is a sign of a viral infection and the body's response to it.[21, 26, 40] AST or aspartate aminotransferase, the most important feature in the tree-based methods, is an enzyme mainly found in heart and liver, its levels increase when the muscles of these organs are injured.[11, 35] This is also the case during a COVID-19 infection since the virus attacks not only the upper respiratory tracts but the whole body including the liver and heart.[42] CRP or C-reactive protein is another substance found during a COVID-19 infection. It is produced in the liver and is discharged after tissue damage, the start of an infection or other inflammatory causes. Increased volumes of this protein are often the first indication of an infection or inflammation in the body.[12, 35] Elevated levels of this protein can also be observed during a COVID-19 infection since it is an infection and primarily targets lung tissue.[18, 21] LDH or lactate dehydrogenase is an enzyme involved in metabolic cycles for energy production, it is present in almost all cells in the body especially in the heart, liver, lungs, kidneys, muscles and blood cells. An increase in LDH can indicate acute kidney or liver disease, hypoxia, or heart and lung infarction.[14, 35] According to [21, 18], a blood test reveals elevated levels of LDH because Sars-CoV-2 primarily attacks the upper respiratory tracts which leads to lung damage and the discharge of LDH into the blood stream. Age as the fourth important feature in the Decision Tree can also be a predictor for a positive result. [33] determines that individuals older than 70 years are more susceptible to a severe course of the disease or even death. Further, the study revealed a higher risk for male individuals. For eosinophils and basophils, [21, 40] reveal a significant decrease for patients with a positive test result. But [21] notes that these differences might not have any clinical implication during diagnosis since the count in healthy individuals is also rather low and exhibits a large variability. In conclusion, the comparison of the most important features of every classifier with the findings from

medical research reveals that the models use feature that medical research deemed as significant to identify patients with COVID-19. Thereby, they can be considered valid regarding their reasoning and classification in a theoretical or laboratory setting.

The two paragraphs above certify the model statistical and theoretical validity, but they lack to prove that these models will also benefit medical personnel in the real world. Relational and ecological validity inspect how a model impacts the clinical workflow and the overall social environment. Specifically, relational validity refers to which extent different user groups, e.g., medical workers or patients, can relate to the model, i.e., how much they trust the predictions of the model [15]. Users can either under-rely on the model ignoring all the predictions presented to them, or over-rely on the model accepting all predictions without questioning them. The former is disadvantageous because in this case the model would not have any benefit in a clinical setting. The latter could be seen as detrimental as this can lead to biased decision making or automation bias which could affect patients negatively [15, 9]. Ecological validity investigates the impact of the technology further scrutinizing the intersection of the clinical and social settings a model is deployed in. A simple way to assess this type of validity is to compare performance-, outcome- and practice-oriented measures of different medical teams utilizing the model and relying on traditional technology in the same setting [9]. Moreover, relational validity also assesses the sustainability of a model by continuously examining the effect of the model over time. As Parikh, Obermeyer, and Navathe [31] notes "unlike a drug or device, algorithms are not static products [as] their inputs [...] can change with context". Accordingly, AI models should be assessed periodically examining if they continue to provide comparable net benefits [9].

4.2   Discussion of Methods

The discussion of the methods is mainly focused on the imputation method MICE since it is a fairly new technique and is not commonly used to impute missing values. In order to asses the imputation procedure, this section will look at which method the imputation model used to impute the missing values and how the imputations compare to the original (non-imputed) data. The `mice()` package in R provides functions to inspect the imputation model used after the imputation is done. Since MICE can handle variables of different types and distributions and due to its individualistic approach, every variable can utilize a different model type to impute the missing values. In our case, the imputation method used the same model type

25

for all variables as a consequence of the non-normality of the data called *Predictive Mean Matching* (PMM). PMM imputes missing values by using a small subset of complete observations called the donor pool. The donor pool contains 3 to 10 donor candidates which exhibit the same or similar predicted values compared to the predicted value of the missing entry. One donor is randomly selected from the candidates, and the observed value of the donor is then used to replace the missing value [7, 2, 29]. It is usually used to model data when the assumptions of normality and homoscedasticity are in questions, as is the case for the data used in this thesis [29].

The imputations of the model can be assessed by generating summary statistics for the observed and the imputed values separately as well as jointly for each variable. Especially comparing the differences in mean and standard deviation between the observed and imputed values of each variable can help identify variables of concern [4]. When comparing the mean of the observed data with the mean of all samples of the imputed sets, most variables exhibit similar values for the summary statistics. Only ALP, GGT, LDH and Neutrophils exhibit apparent deviations from the observed data. It should be noted that most deviations are not significant. When comparing the summary statistics of the observed data and only the imputed values for each data set, there are obvious deviations in every variable. However, it should be noted that with 70% of samples missing at least one feature, it is hard to compare the statistics of the observed values with the imputed ones. Especially, since 117 of the 196 missing samples have a negative test result, which amounts to almost 60% of the missing samples and 42% of all samples, and only 79 of the missing samples have a negative test result. This imbalance is also reflected in the samples where all features are present. Of 83 complete samples only 8 samples have a negative test result and 60 have a positive result. Although the target variable was not available to the imputation model at the time of imputation, the characteristics of the target should have transpired in the data. Since MICE operates on the characteristics of the data, this imbalance could be reflected in the imputation model. As reported in the section above the values for lymphocytes, eosinophils and basophils are decreased in patients who have the disease and therefore also have a positive test result. Inspecting the summary statistics of the imputed sets with this in mind, makes the lower mean and standard deviation more sensible. It should also be noted that ALP and GGT have the highest missing value proportion. Since MICE has less data to base its imputations on, it can be expected that the imputation exhibit apparent deviations from the observed values. MICE also accounts for the uncertainty during the imputation process, meaning a higher number of missing values represents a higher uncertainty and therefore the imputation model is not able to make as educated guesses as for other variables with more observed data.

In conclusion, it is very hard to make statements about the goodness of the imputation model. Most imputed sets do not exhibit drastic deviations from the observed set of observations and for those variables that show apparent deviations it can be ascribed to an imbalance when looking at the samples with missing values. Further, there is no standard procedure to asses the imputations produced by MICE and can therefore be very subjective. Intuitively, the imputations still seem like a fairly good approximation of the data. For further research, I would nonetheless recommend using another method to impute missing values that is more commonly used and has a theoretical basis. For example, Brinati et al. use K-nearest neighbor imputation in a subsequent study [10] which uses a larger data set than the one in [6].

The implementation of MICE used to impute the missing values is, as already mentioned, the R package `mice()` since the sklearn implementation was at the time not able to impute non-normal data correctly. The R implementation, although much better suited, has its own limitation. Namely, it is not able to apply the imputation model to other data only the data it is fitted on. Usually, when using any form of cross-validation the data is split into training and testing data before the imputation is done. The imputation method is then trained on the training data and the trained imputation model is applied to the training as well as the testing data. Using this process, the risk of data leakage is lowered. Data leakage is a term in machine learning that describes the contamination of a model with information from outside the training data where the model could learn something that it could not otherwise [23]. In the context of this thesis, data leakage could take place during the imputation process. Due to the limitation of the R implementation the whole data set is used to fit the imputation model because it is not possible to apply the model to different data sets. Therefore, characteristics from the test data are used to build the imputation for the training data and vice versa. However, the data is split into training and test data after the imputation, consequently lowering the risk of leakage. Moreover, it could be argued that it is not necessarily data leakage as no test data is used to train the classifier themselves but only to perform the imputation. Even if it had been possible to fit the imputation model only on the training data and apply it to both the training and test data, the appropriateness would have been questionable. As MICE is built on the facets of the data, applying the imputation model based on the training data to test data could lead to false or unreliable imputations since the training data does not necessarily carry the characteristics of the test data. Hence, training the imputation model on the whole data set could be advantageous as it would encompass the characteristics of the whole data set. Additionally, training MICE on a very small sample size cannot account for the complex relationships between the features due to the reduced variability and sparseness of the data set. Regardless of the implementation, MICE is also not

a commonly used imputation method. Thus, there are no guidelines or procedure to identify a good imputations. Further, MICE lacks a theoretical basis since fitting a series of conditional probabilities may not be consistent with a proper joint distribution [4]. The method relies on empirical studies rather than a theoretical basis to justify its procedure. In practice, however, this may not be a large issue, but further research is needed here. Despite these shortcomings, MICE provides a great advantage over other missing data techniques in terms of flexibility regarding variable type and number of variables to impute [4, 44]. After all, MICE should be used where traditional imputation methods face their limits due to small sample size and where the characteristics of the variables and their relations are still recognizable.

Another explanation for the differing results of this re-implementation is the way the authors provided information on their implementation of the model training and selection process. Namely, they did not provide detailed information about which hyperparameters were tuned during cross-validation nor their ranges. Further, the structure of the cross-validation process was not clear at all times.
Moreover, Brinati et al. do not report all evaluation metrics used to determine the best classifiers. They only report 95% confidence intervals for the average accuracy and balanced accuracy as well as point references for the classifiers they deemed as best performing. There was no further information on other evaluation metrics like sensitivity or AUC. Additionally, the authors did only provide the configuration for one of the best performing models, namely the Random Forest. Unfortunately, this did not inform about the ranges for each hyperparameter used during Grid Search. Nevertheless, the authors did provide their data and a description of each variable in the data set. It should also be noted that [6] was only a feasibility study to explore if machine learning classifiers can help identify patients with COVID-19 solely based on a routine blood exam where the focus was not on replicability but feasibility. However, research like this that has a potential effect on an individual's health should strive to be as transparent and comprehensible as possible.

4.3 Conclusion

In conclusion, this thesis replicates two of the eight classifiers in [6]. The classifiers predict the outcome of a PCR test for COVID-19 using a routine blood exam. Although the classifiers perform worse than in the original paper, they still can be regarded as substantial due to a 90% sensitivity and an accuracy above 70% for both classifiers. Further, a Decision Tree model was built to give a graphical representation of a possible classification reasoning. A comparison with findings

from medical research revealed that features identified as most important by the classifiers were also deemed pivotal in diagnosing COVID-19. Thereby, confirming the patterns found by the classifiers and certifying them a theoretical validity. This implementation used Multiple Imputation using Chained Equations to impute the missing values. This method was used due to the small sample size of 279 individuals and the proportionally high rate of sampels with at least one missing value. Though MICE lacks a theoretical basis and justifies its procedure with experimental studies, it provides great advantages especially where sample size is too small for more conventional and theoretically justified imputation methods and where the variables differ in terms of their type and distribution. Seeing that the replicated paper was a feasibility study investigating if it is possible to predict a PCR test result from a range of blood values, further research should be done on this topic. For instance, Brinati et al. did a follow up study using a data set comprising more samples, more blood values and symptomatic observations at the time of triage or admittance to a hospital [10]. Importantly, it should always be brought to attention that these kind of models should never replace the actual medical test. They should be seen as a valuable though non-conclusive tool to detect patients with a certain disease earlier and better, resulting in improved management of these patients while awaiting confirmation by the medical test.

Code & Data Availability

The code and data used to train the classifiers is made available at the GitHub repository https://github.com/lschiesser/ba. The data set is also available at the original source https://zenodo.org/record/3886927#.YBPnRXkxlEY.
A data drive with the code and data was submitted along a hard copy version of this thesis to the examination office.

Declaration

I declare that...

Appendix A

Supplementary Tables

Feature	Data Type
Gender	Categorical
Age	Numerical (discrete)
WBC (White blood cell count)	Numerical (continuous)
Platelets	Numerical (continuous)
Neutrophils	Numerical (continuous)
Lymphocytes	Numerical (continuous)
Monocytes	Numerical (continuous)
Eosinophils	Numerical (continuous)
Basophils	Numerical (continuous)
CRP (C-reactive protein)	Numerical (continuous)
AST (aspartate aminotransferase)	Numerical (continuous)
ALT (alanine aminotransferase)	Numerical (continuous)
ALP (alkaline phosphatase)	Numerical (continuous)
GGT (gamma glutamyl transferase)	Numerical (continuous)
LDH (lactate dehydrogenase)	Numerical (continuous)
SWAB	Categorical

Table A.1: Overview of all features of the data set

Feature	Unit	Mean	Std	Median
Age	Years	61.33	18.05	64
White Blood Cell Count (WBC)	10^9/L	8.49	4.89	7.10
Platelets	10^9/L	224.91	102.61	204.00
Neutrophils	10^9/L	4.64	4.50	3.90
Lymphocytes	10^9/L	0.88	0.87	0.80
Monocytes	10^9/L	0.45	0.44	0.40
Eosinophils	10^9/L	0.04	0.12	0.00
Basophils	10^9/L	0.01	0.03	0.00
C-reactive protein (CRP)	mg/L	88.93	94.32	53.10
Aspartate Aminotransferase (AST)	U/L	53.81	57.59	36.00
Alanine Aminotransferase (ALT)	U/L	42.82	45.43	30.00
Alkaline Phosphatase (ALP)	U/L	42.21	75.71	68.00
Gamma Glutamyl Transferase (GGT)	U/L	40.20	101.29	0.00
Lactate dehydrogenase (LDH)	U/L	264.54	238.53	254.00

Table A.2: Descriptive statistics for numerical features in data set (including missing values as in [6])

Feature	Number of NaN (in %)
Gender	0 (0 %)
Age	2 (0.72 %)
WBC (White blood cell count)	2 (0.72 %)
Platelets	2 (0.72 %)
Neutrophils	70 (25.09 %)
Lymphocytes	71 (25.45 %)
Monocytes	70 (25.09 %)
Eosinophils	70 (25.09 %)
Basophils	71 (25.45 %)
CRP (C-reactive protein)	6 (2.15 %)
AST (aspartate aminotransferase)	2 (0.72 %)
ALT (alanine aminotransferase)	13 (4.66 %)
ALP (alkaline phosphatase)	148 (53.05 %)
GGT (gamma glutamyl transferase)	143 (51.25 %)
LDH (lactate dehydrogenase)	85 (30.47 %)
SWAB	0 (0 %)

Table A.3: Number of missing values and their proportion of the total number of data points

Feature	Unit	Mean	Std	Median
Age	Years	61.78	17.81	64
White Blood Cell Count (WBC)	10^9/L	8.55	4.86	7.10
Platelets	10^9/L	226.5	101.2	205.00
Neutrophils	10^9/L	6.20	4.17	5.10
Lymphocytes	10^9/L	1.19	0.80	1.00
Monocytes	10^9/L	0.61	0.41	0.50
Eosinophils	10^9/L	0.06	0.13	0.00
Basophils	10^9/L	0.01	0.04	0.00
C-reactive protein (CRP)	mg/L	90.89	94.42	54.20
Aspartate Aminotransferase (AST)	U/L	54.20	57.61	36.00
Alanine Aminotransferase (ALT)	U/L	44.92	45.50	31.00
Alkaline Phosphatase (ALP)	U/L	89.89	89.09	71.00
Gamma Glutamyl Transferase (GGT)	U/L	82.48	132.70	41.00
Lactate dehydrogenase (LDH)	U/L	380.45	193.98	328.00

Table A.4: Descriptive statistics for numerical features in data set (excluding missing values)

Feature	Test statistic	p-value
Age	0.976	0.000
WBC (White blood cell count)	0.873	0.000
Platelets	0.930	0.000
Neutrophils	0.838	0.000
Lymphocytes	0.785	0.000
Monocytes	0.811	0.000
Eosinophils	0.457	0.000
Basophils	0.395	0.000
CRP (C-reactive protein)	0.836	0.000
AST (aspartate aminotransferase)	0.556	0.000
ALT (alanine aminotransferase)	0.629	0.000
ALP (alkaline phosphatase)	0.420	0.000
GGT (gamma glutamyl transferase)	0.500	0.000
LDH (lactate dehydrogenase)	0.877	0.000

Table A.5: Results of Shapiro-Wilk test for normality for numerical features of the data set

	Fold1		Fold2		Fold3		Fold4		Fold5		Combined	
	mean	std	mean	std	mean	std	mean	std	mean	std	mean	std
RF	0.72	0.01	0.84	0.03	0.81	0.03	0.75	0.03	0.77	0.03	0.78	0.05
LR	0.71	0.03	0.81	0.02	0.74	0.03	0.70	0.06	0.73	0.04	0.74	0.05

Table A.6: Mean training accuracies and their standard deviations (std) for each training fold and all training folds combined. Random Forest = RF, Logisitic Regression = LR

	Fold1		Fold2		Fold3		Fold4		Fold5		Combined	
	mean	std	mean	std	mean	std	mean	std	mean	std	mean	std
RF	0.69	0.01	0.81	0.04	0.79	0.03	0.73	0.03	0.71	0.04	0.75	0.05
LR	0.67	0.02	0.78	0.03	0.72	0.03	0.68	0.06	0.67	0.04	0.70	0.06

Table A.7: Mean training balanced accuracies and their standard deviations (std) for each training fold and all training folds combined. Random Forest = RF, Logisitic Regression = LR

Model	acc	b_acc	sensitivity	specificity	ppv	auc	a_precision
RF	0.768	0.737	0.909	0.565	0.750	0.802	0.829
LR	0.732	0.694	0.909	0.478	0.714	0.808	0.855
DT	0.714	0.685	0.848	0.522	0.718	0.685	0.698

Table A.8: Validation metrics for all classifiers; RF = Random Forest, DT = Decision Tree, LR = Logisitic Regression

Fold	Imputed Set	Model	Model Count	acc	b_acc	sensitivity	specificity	ppv	auc
0	1	lr	0	0.750	0.709	0.939	0.478	0.721	0.816
0	2	lr	1	0.714	0.679	0.879	0.478	0.707	0.837
0	3	lr	2	0.696	0.663	0.848	0.478	0.700	0.806
0	4	lr	3	0.696	0.663	0.848	0.478	0.700	0.797
0	5	lr	4	0.679	0.642	0.848	0.435	0.683	0.826
1	1	lr	5	0.804	0.787	0.825	0.750	0.892	0.845
1	2	lr	6	0.839	0.831	0.850	0.812	0.919	0.872
1	3	lr	7	0.804	0.787	0.825	0.750	0.892	0.856
1	4	lr	8	0.786	0.738	0.850	0.625	0.850	0.822
1	5	lr	9	0.804	0.769	0.850	0.688	0.872	0.833
2	1	lr	10	0.732	0.713	0.818	0.609	0.750	0.742
2	2	lr	11	0.768	0.750	0.848	0.652	0.778	0.764
2	3	lr	12	0.768	0.757	0.818	0.696	0.794	0.823
2	4	lr	13	0.732	0.720	0.788	0.652	0.765	0.773
2	5	lr	14	0.696	0.683	0.758	0.609	0.735	0.758
3	1	lr	15	0.714	0.695	0.771	0.619	0.771	0.774
3	2	lr	16	0.750	0.733	0.800	0.667	0.800	0.788
3	3	lr	17	0.643	0.619	0.714	0.524	0.714	0.686
3	4	lr	18	0.750	0.733	0.800	0.667	0.800	0.777
3	5	lr	19	0.625	0.605	0.686	0.524	0.706	0.680
4	1	lr	20	0.800	0.723	0.972	0.474	0.778	0.801
4	2	lr	21	0.727	0.680	0.833	0.526	0.769	0.781
4	3	lr	22	0.709	0.629	0.889	0.368	0.727	0.773
4	4	lr	23	0.691	0.627	0.833	0.421	0.732	0.754
4	5	lr	24	0.727	0.680	0.833	0.526	0.769	0.785
0	1	rf	0	0.732	0.694	0.909	0.478	0.714	0.792
0	2	rf	1	0.714	0.685	0.848	0.522	0.718	0.801
0	3	rf	2	0.732	0.694	0.909	0.478	0.714	0.782
0	4	rf	3	0.732	0.700	0.879	0.522	0.725	0.739
0	5	rf	4	0.714	0.692	0.818	0.565	0.730	0.760
1	1	rf	5	0.875	0.856	0.900	0.812	0.923	0.848
1	2	rf	6	0.821	0.800	0.850	0.750	0.895	0.842
1	3	rf	7	0.839	0.812	0.875	0.750	0.897	0.850
1	4	rf	8	0.839	0.812	0.875	0.750	0.897	0.809
1	5	rf	9	0.804	0.750	0.875	0.625	0.854	0.806
2	1	rf	10	0.804	0.787	0.879	0.696	0.806	0.825
2	2	rf	11	0.857	0.839	0.939	0.739	0.838	0.839
2	3	rf	12	0.786	0.772	0.848	0.696	0.800	0.816
2	4	rf	13	0.804	0.781	0.909	0.652	0.789	0.847
2	5	rf	14	0.804	0.787	0.879	0.696	0.806	0.831
3	1	rf	15	0.750	0.714	0.857	0.571	0.769	0.826
3	2	rf	16	0.696	0.700	0.686	0.714	0.800	0.783
3	3	rf	17	0.768	0.738	0.857	0.619	0.789	0.848
3	4	rf	18	0.786	0.762	0.857	0.667	0.811	0.812
3	5	rf	19	0.768	0.729	0.886	0.571	0.775	0.793
4	1	rf	20	0.782	0.734	0.889	0.579	0.800	0.836
4	2	rf	21	0.764	0.695	0.917	0.474	0.767	0.798
4	3	rf	22	0.727	0.655	0.889	0.421	0.744	0.848
4	4	rf	23	0.764	0.708	0.889	0.526	0.780	0.798
4	5	rf	24	0.800	0.760	0.889	0.632	0.821	0.777

Table A.9: Evaluation metrics for Random Forest (rf) and Logisitc Regression (lr) during the nested cross validation

	AGE		WBC		Platelets		Neutrophils		Lymphocytes		Monocytes		Eosinophils		Basophils		CRP		AST		ALT		ALP		GGT		LDH	
	mean	std	mean	std	mean	std	mean	std	mean	std	mean	std	mean	std	mean	std	mean	std	mean	std	mean	std	mean	std	mean	std	mean	std
original	61.776	17.816	8.553	4.855	226.532	101.174	6.200	4.173	1.187	0.806	0.606	0.410	0.055	0.132	0.014	0.039	90.889	94.421	54.202	57.613	44.917	45.503	89.893	89.090	82.478	132.703	380.448	193.984
1.0	61.839	17.773	8.574	4.863	226.654	100.820	6.597	4.482	1.260	0.899	0.649	0.455	0.066	0.147	0.017	0.041	92.581	96.875	54.208	57.458	47.459	49.868	82.362	66.091	79.681	119.072	379.516	199.693
2.0	61.832	17.768	8.557	4.840	225.951	101.067	6.597	4.301	1.236	0.807	0.655	0.458	0.052	0.140	0.015	0.039	91.247	94.973	54.269	57.422	47.405	50.648	81.803	65.194	73.470	103.199	365.706	178.115
3.0	61.871	17.792	8.600	4.870	226.288	100.896	6.650	4.439	1.220	0.801	0.659	0.473	0.054	0.123	0.014	0.038	91.278	94.059	54.161	57.417	46.774	48.087	83.484	67.061	75.283	106.761	367.760	191.073
4.0	61.728	17.768	8.557	4.839	226.571	100.911	6.625	4.353	1.209	0.799	0.643	0.429	0.054	0.124	0.016	0.043	91.447	94.246	54.029	57.452	46.864	48.285	83.065	66.928	76.444	117.722	374.405	196.479
5.0	61.832	17.806	8.534	4.843	226.446	101.323	6.592	4.412	1.260	0.899	0.649	0.455	0.055	0.126	0.015	0.039	91.255	94.812	54.004	57.453	45.943	45.804	83.964	67.706	75.384	113.305	374.771	195.309
6.0	61.839	17.773	8.574	4.863	226.654	100.820	6.597	4.482	1.260	0.899	0.649	0.455	0.066	0.147	0.017	0.041	92.581	96.875	54.208	57.458	47.459	49.868	82.362	66.091	79.681	119.072	379.516	199.693
7.0	61.832	17.768	8.557	4.840	225.951	101.067	6.597	4.301	1.236	0.807	0.655	0.458	0.052	0.140	0.015	0.039	91.247	94.973	54.269	57.422	47.405	50.648	81.803	65.194	73.470	103.199	365.706	178.115
8.0	61.871	17.792	8.600	4.870	226.288	100.896	6.650	4.439	1.220	0.801	0.659	0.473	0.054	0.123	0.014	0.038	91.278	94.059	54.161	57.417	46.774	48.087	83.484	67.061	75.283	106.761	367.760	191.073
9.0	61.728	17.768	8.557	4.839	226.571	100.911	6.625	4.353	1.209	0.799	0.643	0.429	0.054	0.124	0.016	0.043	91.447	94.246	54.029	57.452	46.864	48.285	83.065	66.928	76.444	117.722	374.405	196.479
10.0	61.832	17.806	8.534	4.843	226.446	101.323	6.592	4.412	1.260	0.899	0.642	0.446	0.055	0.126	0.015	0.039	91.255	94.812	54.208	57.453	45.943	45.804	83.964	67.706	75.384	113.305	374.771	195.309
11.0	61.839	17.773	8.574	4.863	226.654	101.067	6.597	4.482	1.236	0.899	0.649	0.458	0.066	0.147	0.017	0.041	92.581	96.875	54.269	57.458	47.459	49.868	82.362	66.091	79.681	119.072	379.516	199.693
12.0	61.832	17.768	8.557	4.840	225.951	100.896	6.650	4.301	1.220	0.807	0.655	0.473	0.052	0.140	0.014	0.039	91.247	94.973	54.161	57.422	46.774	50.648	83.065	65.194	73.470	103.199	365.706	178.115
13.0	61.871	17.792	8.600	4.870	226.288	100.911	6.625	4.439	1.229	0.801	0.659	0.429	0.054	0.123	0.016	0.038	91.447	94.059	54.029	57.417	45.943	48.087	83.484	67.061	75.384	106.761	367.760	191.073
14.0	61.728	17.768	8.557	4.839	226.571	100.820	6.597	4.353	1.209	0.799	0.643	0.446	0.054	0.124	0.015	0.043	91.255	94.246	54.004	57.452	47.405	48.285	83.964	66.928	76.444	117.722	374.405	196.479
15.0	61.832	17.806	8.534	4.843	226.446	101.323	6.592	4.412	1.260	0.899	0.649	0.455	0.055	0.126	0.017	0.039	91.247	94.973	54.269	57.422	47.405	50.648	81.803	67.706	73.470	119.072	379.516	199.693
16.0	61.839	17.773	8.574	4.863	226.654	100.820	6.597	4.482	1.260	0.899	0.649	0.455	0.066	0.147	0.017	0.041	92.581	96.875	54.208	57.458	47.459	49.868	82.362	66.091	79.681	119.072	379.516	199.693
17.0	61.832	17.768	8.557	4.840	225.951	101.067	6.597	4.301	1.236	0.807	0.655	0.458	0.052	0.140	0.015	0.039	91.247	94.973	54.269	57.422	47.405	50.648	81.803	65.194	73.470	103.199	365.706	178.115
18.0	61.871	17.792	8.600	4.870	226.288	100.896	6.650	4.439	1.220	0.801	0.659	0.473	0.054	0.123	0.014	0.038	91.278	94.059	54.161	57.417	46.774	48.087	83.484	67.061	75.283	106.761	367.760	191.073
19.0	61.728	17.768	8.557	4.839	226.571	100.911	6.625	4.353	1.229	0.807	0.643	0.429	0.054	0.124	0.016	0.043	91.447	94.246	54.029	57.452	46.864	48.285	83.065	66.928	75.384	113.305	374.405	195.309
20.0	61.832	17.806	8.534	4.843	226.446	101.323	6.592	4.412	1.209	0.799	0.642	0.446	0.055	0.126	0.015	0.039	91.255	94.812	54.004	57.453	45.943	45.804	83.964	67.706	76.444	117.722	374.405	196.479
21.0	61.839	17.773	8.574	4.863	226.654	100.820	6.597	4.482	1.260	0.899	0.649	0.455	0.066	0.147	0.017	0.041	92.581	96.875	54.208	57.458	47.459	49.868	82.362	66.091	79.681	119.072	379.516	199.693
22.0	61.871	17.768	8.557	4.840	225.951	101.067	6.597	4.301	1.236	0.807	0.655	0.458	0.052	0.140	0.014	0.039	91.247	94.973	54.161	57.422	46.774	50.648	81.803	65.194	75.283	103.199	365.706	178.115
23.0	61.871	17.792	8.600	4.870	226.288	100.896	6.650	4.439	1.220	0.801	0.659	0.473	0.054	0.123	0.014	0.038	91.278	94.059	54.161	57.417	46.774	48.087	83.484	67.061	75.283	106.761	367.760	191.073
24.0	61.728	17.768	8.557	4.839	226.571	100.911	6.625	4.353	1.229	0.807	0.643	0.429	0.054	0.124	0.016	0.043	91.447	94.246	54.029	57.452	46.864	48.285	83.065	66.928	75.384	113.305	374.771	195.309
25.0	61.832	17.806	8.534	4.843	226.446	101.323	6.592	4.412	1.209	0.799	0.642	0.446	0.055	0.126	0.015	0.039	91.255	94.812	54.004	57.453	45.943	45.804	83.964	67.706	76.444	117.722	374.405	196.479

Table A.10: Numerical summaries for all variables of the original not-imputed data set (denoted by original) and the imputed data sets (denoted by a number)

Table A.11: Numerical summaries for all variables of the original not-imputed data set (denoted by original) and the imputed data sets (denoted by a number) only for the imputed values

	AGE		WBC		Platelets		Neutrophils		Lymphocytes		Monocytes		Eosinophils		Basophils		CRP		AST		ALT		ALP		GGT		LDH	
	mean	std	mean	std	mean	std	mean	std	mean	std	mean	std	mean	std	mean	std	mean	std	mean	std	mean	std	mean	std	mean	std	mean	std
original	61.776	17.816	8.553	4.855	226.532	101.174	6.200	4.173	1.187	0.806	0.606	0.410	0.055	0.132	0.014	0.039	90.889	94.421	54.202	57.613	44.917	45.503	89.893	89.090	82.478	132.703	380.448	193.984
1.0	70.500	7.778	11.500	7.071	243.500	2.121	7.783	5.153	1.475	1.105	0.780	0.553	0.099	0.182	0.025	0.044	169.583	171.826	55.000	41.012	99.462	93.888	75.696	33.854	77.021	104.884	377.388	213.331
2.0	69.500	6.364	9.100	2.404	145.500	37.477	7.783	4.488	1.382	0.795	0.803	0.557	0.043	0.161	0.017	0.038	107.533	127.200	63.500	19.092	98.308	103.728	74.642	30.147	64.902	62.903	332.059	129.954
3.0	75.000	7.071	15.150	0.778	192.500	50.205	7.993	4.947	1.320	0.784	0.817	0.600	0.051	0.088	0.014	0.035	109.000	80.700	48.500	17.678	84.769	78.776	77.811	37.641	68.441	73.996	338.800	182.065
4.0	55.000	8.485	9.050	1.485	232.000	74.953	7.891	4.659	1.352	0.800	0.754	0.468	0.050	0.097	0.023	0.051	116.850	89.815	30.000	18.385	86.692	80.529	77.020	37.065	68.636	91.091	361.812	198.849
5.0	69.500	20.506	5.900	0.566	214.500	168.999	7.760	4.910	1.273	0.779	0.750	0.527	0.056	0.104	0.017	0.038	107.900	120.274	26.500	3.536	66.923	48.786	78.716	39.890	70.706	101.595	360.612	202.547
6.0	70.500	7.778	11.500	7.071	243.500	2.121	7.783	5.153	1.475	1.105	0.780	0.553	0.099	0.182	0.025	0.044	169.583	171.826	55.000	41.012	99.462	93.888	75.696	33.854	77.021	104.884	377.388	213.331
7.0	69.500	6.364	9.100	2.404	145.500	37.477	7.783	4.488	1.382	0.795	0.803	0.557	0.043	0.161	0.017	0.038	107.533	127.200	63.500	19.092	98.308	103.728	74.642	30.147	64.902	62.903	332.059	129.954
8.0	75.000	7.071	15.150	0.778	192.500	50.205	7.993	4.947	1.320	0.784	0.817	0.600	0.051	0.088	0.014	0.035	109.000	80.700	48.500	17.678	84.769	78.776	77.811	37.641	68.441	73.996	338.800	182.065
9.0	55.000	8.485	9.050	1.485	232.000	74.953	7.891	4.659	1.352	0.800	0.754	0.468	0.050	0.097	0.023	0.051	116.850	89.815	30.000	18.385	86.692	80.529	77.020	37.065	68.636	91.091	361.812	198.849
10.0	69.500	20.506	5.900	0.566	214.500	168.999	7.760	4.910	1.273	0.779	0.750	0.527	0.056	0.104	0.017	0.038	107.900	120.274	26.500	3.536	66.923	48.786	78.716	39.890	70.706	101.595	360.612	202.547
11.0	70.500	7.778	11.500	7.071	243.500	2.121	7.783	5.153	1.475	1.105	0.780	0.553	0.099	0.182	0.025	0.044	169.583	171.826	55.000	41.012	99.462	93.888	75.696	33.854	77.021	104.884	377.388	213.331
12.0	69.500	6.364	9.100	2.404	145.500	37.477	7.783	4.488	1.382	0.795	0.803	0.557	0.043	0.161	0.017	0.038	107.533	127.200	63.500	19.092	98.308	103.728	74.642	30.147	64.902	62.903	332.059	129.954
13.0	75.000	7.071	15.150	0.778	192.500	50.205	7.993	4.947	1.320	0.784	0.817	0.600	0.051	0.088	0.014	0.035	109.000	80.700	48.500	17.678	84.769	78.776	77.811	37.641	68.441	73.996	338.800	182.065
14.0	55.000	8.485	9.050	1.485	232.000	74.953	7.891	4.659	1.352	0.800	0.754	0.468	0.050	0.097	0.023	0.051	116.850	89.815	30.000	18.385	86.692	80.529	77.020	37.065	68.636	91.091	361.812	198.849
15.0	69.500	20.506	5.900	0.566	214.500	168.999	7.760	4.910	1.273	0.779	0.750	0.527	0.056	0.104	0.017	0.038	107.900	120.274	26.500	3.536	66.923	48.786	78.716	39.890	70.706	101.595	360.612	202.547
16.0	70.500	7.778	11.500	7.071	243.500	2.121	7.783	5.153	1.475	1.105	0.780	0.553	0.099	0.182	0.025	0.044	169.583	171.826	55.000	41.012	99.462	93.888	75.696	33.854	77.021	104.884	377.388	213.331
17.0	69.500	6.364	9.100	2.404	145.500	37.477	7.783	4.488	1.382	0.795	0.803	0.557	0.043	0.161	0.017	0.038	107.533	127.200	63.500	19.092	98.308	103.728	74.642	30.147	64.902	62.903	332.059	129.954
18.0	75.000	7.071	15.150	0.778	192.500	50.205	7.993	4.947	1.320	0.784	0.817	0.600	0.051	0.088	0.014	0.035	109.000	80.700	48.500	17.678	84.769	78.776	77.811	37.641	68.441	73.996	338.800	182.065
19.0	55.000	8.485	9.050	1.485	232.000	74.953	7.891	4.659	1.352	0.800	0.754	0.468	0.050	0.097	0.023	0.051	116.850	89.815	30.000	18.385	86.692	80.529	77.020	37.065	68.636	91.091	361.812	198.849
20.0	69.500	20.506	5.900	0.566	214.500	168.999	7.760	4.910	1.273	0.779	0.750	0.527	0.056	0.104	0.017	0.038	107.900	120.274	26.500	3.536	66.923	48.786	78.716	39.890	70.706	101.595	360.612	202.547
21.0	70.500	7.778	11.500	7.071	243.500	2.121	7.783	5.153	1.475	1.105	0.780	0.553	0.099	0.182	0.025	0.044	169.583	171.826	55.000	41.012	99.462	93.888	75.696	33.854	77.021	104.884	377.388	213.331
22.0	69.500	6.364	9.100	2.404	145.500	37.477	7.783	4.488	1.382	0.795	0.803	0.557	0.043	0.161	0.017	0.038	107.533	127.200	63.500	19.092	98.308	103.728	74.642	30.147	64.902	62.903	332.059	129.954
23.0	75.000	7.071	15.150	0.778	192.500	50.205	7.993	4.947	1.320	0.784	0.817	0.600	0.051	0.088	0.014	0.035	109.000	80.700	48.500	17.678	84.769	78.776	77.811	37.641	68.441	73.996	338.800	182.065
24.0	55.000	8.485	9.050	1.485	232.000	74.953	7.891	4.659	1.352	0.800	0.754	0.468	0.050	0.097	0.023	0.051	116.850	89.815	30.000	18.385	86.692	80.529	77.020	37.065	68.636	91.091	361.812	198.849
25.0	69.500	20.506	5.900	0.566	214.500	168.999	7.760	4.910	1.273	0.779	0.750	0.527	0.056	0.104	0.017	0.038	107.900	120.274	26.500	3.536	66.923	48.786	78.716	39.890	70.706	101.595	360.612	202.547

	AGE		WBC		Platelets		Neutrophils		Lymphocytes		Monocytes		Eosinophils		Basophils		CRP		AST		ALT		ALP		GGT		LDH	
	test value	p-value	test value	p-value	test value	p-value	test value	p-value	test value	p-value	test value	p-value	test value	p-value	test value	p-value	test value	p-value	test value	p-value	test value	p-value	test value	p-value	test value	p-value	test value	p-value
1.0	38718.000	0.458	38732.000	0.461	38733.000	0.461	30379.000	0.000	30061.500	0.000	30729.500	0.000	30660.500	0.000	29885.000	0.000	38342.000	0.381	38666.500	0.447	37888.000	0.294	17693.000	0.000	19648.500	0.000	26864.000	0.000
2.0	38703.500	0.455	38721.000	0.458	38473.500	0.407	30854.000	0.000	30282.000	0.000	30930.500	0.000	28607.000	0.000	29264.000	0.000	38089.500	0.331	38773.000	0.469	37885.500	0.293	17909.000	0.000	18885.500	0.000	26091.000	0.000
3.0	38765.500	0.468	38856.000	0.487	38596.000	0.432	30726.500	0.000	29883.000	0.000	30951.500	0.000	29462.500	0.000	29057.000	0.000	38281.500	0.369	38709.000	0.456	37739.000	0.268	17950.000	0.000	19372.000	0.000	25764.500	0.000
4.0	38558.000	0.425	38723.500	0.459	38672.500	0.448	30807.500	0.000	29886.000	0.000	30569.500	0.000	29206.000	0.000	29485.000	0.000	38241.500	0.361	38546.500	0.422	37666.500	0.255	17898.000	0.000	18751.500	0.000	26550.000	0.000
5.0	38711.500	0.456	38558.000	0.425	38618.500	0.437	30627.000	0.000	29492.500	0.000	30492.000	0.000	29425.000	0.000	29264.000	0.000	38108.500	0.335	38506.500	0.414	37637.000	0.250	18166.500	0.000	18797.000	0.000	26349.000	0.000
6.0	38718.000	0.458	38732.000	0.461	38733.000	0.461	30379.000	0.000	30061.500	0.000	30729.500	0.000	30660.500	0.000	29885.000	0.000	38342.000	0.381	38666.500	0.447	37888.000	0.294	17693.000	0.000	19648.500	0.000	26864.000	0.000
7.0	38703.500	0.455	38721.000	0.458	38473.500	0.407	30854.000	0.000	30282.000	0.000	30930.500	0.000	28607.000	0.000	29264.000	0.000	38089.500	0.331	38773.000	0.469	37885.500	0.293	17909.000	0.000	18885.500	0.000	26091.000	0.000
8.0	38765.500	0.468	38856.000	0.487	38596.000	0.432	30726.500	0.000	29883.000	0.000	30951.500	0.000	29462.500	0.000	29057.000	0.000	38281.500	0.369	38709.000	0.456	37739.000	0.268	17950.000	0.000	19372.000	0.000	25764.500	0.000
9.0	38558.000	0.425	38723.500	0.459	38672.500	0.448	30807.500	0.000	29886.000	0.000	30569.500	0.000	29206.000	0.000	29485.000	0.000	38241.500	0.361	38546.500	0.422	37666.500	0.255	17898.000	0.000	18751.500	0.000	26550.000	0.000
10.0	38711.500	0.456	38558.000	0.425	38618.500	0.437	30627.000	0.000	29492.500	0.000	30492.000	0.000	29425.000	0.000	29264.000	0.000	38108.500	0.335	38506.500	0.414	37637.000	0.250	18166.500	0.000	18797.000	0.000	26349.000	0.000
11.0	38718.000	0.458	38732.000	0.461	38733.000	0.461	30379.000	0.000	30061.500	0.000	30729.500	0.000	30660.500	0.000	29885.000	0.000	38342.000	0.381	38666.500	0.447	37888.000	0.294	17693.000	0.000	19648.500	0.000	26864.000	0.000
12.0	38703.500	0.455	38721.000	0.458	38473.500	0.407	30854.000	0.000	30282.000	0.000	30930.500	0.000	28607.000	0.000	29264.000	0.000	38089.500	0.331	38773.000	0.469	37885.500	0.293	17909.000	0.000	18885.500	0.000	26091.000	0.000
13.0	38765.500	0.468	38856.000	0.487	38596.000	0.432	30726.500	0.000	29883.000	0.000	30951.500	0.000	29462.500	0.000	29057.000	0.000	38281.500	0.369	38709.000	0.456	37739.000	0.268	17950.000	0.000	19372.000	0.000	25764.500	0.000
14.0	38558.000	0.425	38723.500	0.459	38672.500	0.448	30807.500	0.000	29886.000	0.000	30569.500	0.000	29206.000	0.000	29485.000	0.000	38241.500	0.361	38546.500	0.422	37666.500	0.255	17898.000	0.000	18751.500	0.000	26550.000	0.000
15.0	38711.500	0.456	38558.000	0.425	38618.500	0.437	30627.000	0.000	29492.500	0.000	30492.000	0.000	29425.000	0.000	29264.000	0.000	38108.500	0.335	38506.500	0.414	37637.000	0.250	18166.500	0.000	18797.000	0.000	26349.000	0.000
16.0	38718.000	0.458	38732.000	0.461	38733.000	0.461	30379.000	0.000	30061.500	0.000	30729.500	0.000	30660.500	0.000	29885.000	0.000	38342.000	0.381	38666.500	0.447	37888.000	0.294	17693.000	0.000	19648.500	0.000	26864.000	0.000
17.0	38703.500	0.455	38721.000	0.458	38473.500	0.407	30854.000	0.000	30282.000	0.000	30930.500	0.000	28607.000	0.000	29264.000	0.000	38089.500	0.331	38773.000	0.469	37885.500	0.293	17909.000	0.000	18885.500	0.000	26091.000	0.000
18.0	38765.500	0.468	38856.000	0.487	38596.000	0.432	30726.500	0.000	29883.000	0.000	30951.500	0.000	29462.500	0.000	29057.000	0.000	38281.500	0.369	38709.000	0.456	37739.000	0.268	17950.000	0.000	19372.000	0.000	25764.500	0.000
19.0	38558.000	0.425	38723.500	0.459	38672.500	0.448	30807.500	0.000	29886.000	0.000	30569.500	0.000	29206.000	0.000	29485.000	0.000	38241.500	0.361	38546.500	0.422	37666.500	0.255	17898.000	0.000	18751.500	0.000	26550.000	0.000
20.0	38711.500	0.456	38558.000	0.425	38618.500	0.437	30627.000	0.000	29492.500	0.000	30492.000	0.000	29425.000	0.000	29264.000	0.000	38108.500	0.335	38506.500	0.414	37637.000	0.250	18166.500	0.000	18797.000	0.000	26349.000	0.000
21.0	38718.000	0.458	38732.000	0.461	38733.000	0.461	30379.000	0.000	30061.500	0.000	30729.500	0.000	30660.500	0.000	29885.000	0.000	38342.000	0.381	38666.500	0.447	37888.000	0.294	17693.000	0.000	19648.500	0.000	26864.000	0.000
22.0	38703.500	0.455	38721.000	0.458	38473.500	0.407	30854.000	0.000	30282.000	0.000	30930.500	0.000	28607.000	0.000	29264.000	0.000	38089.500	0.331	38773.000	0.469	37885.500	0.293	17909.000	0.000	18885.500	0.000	26091.000	0.000
23.0	38765.500	0.468	38856.000	0.487	38596.000	0.432	30726.500	0.000	29883.000	0.000	30951.500	0.000	29462.500	0.000	29057.000	0.000	38281.500	0.369	38709.000	0.456	37739.000	0.268	17950.000	0.000	19372.000	0.000	25764.500	0.000
24.0	38558.000	0.425	38723.500	0.459	38672.500	0.448	30807.500	0.000	29886.000	0.000	30569.500	0.000	29206.000	0.000	29485.000	0.000	38241.500	0.361	38546.500	0.422	37666.500	0.255	17898.000	0.000	18751.500	0.000	26550.000	0.000
25.0	38711.500	0.456	38558.000	0.425	38618.500	0.437	30627.000	0.000	29492.500	0.000	30492.000	0.000	29425.000	0.000	29264.000	0.000	38108.500	0.335	38506.500	0.414	37637.000	0.250	18166.500	0.000	18797.000	0.000	26349.000	0.000

Table A.12: Results of Mann-Whitney-U test for each variable in each imputed data set; a p-value smaller then 0.05 signals that the imputed variable and the observed values of the variable come from the same distirbution
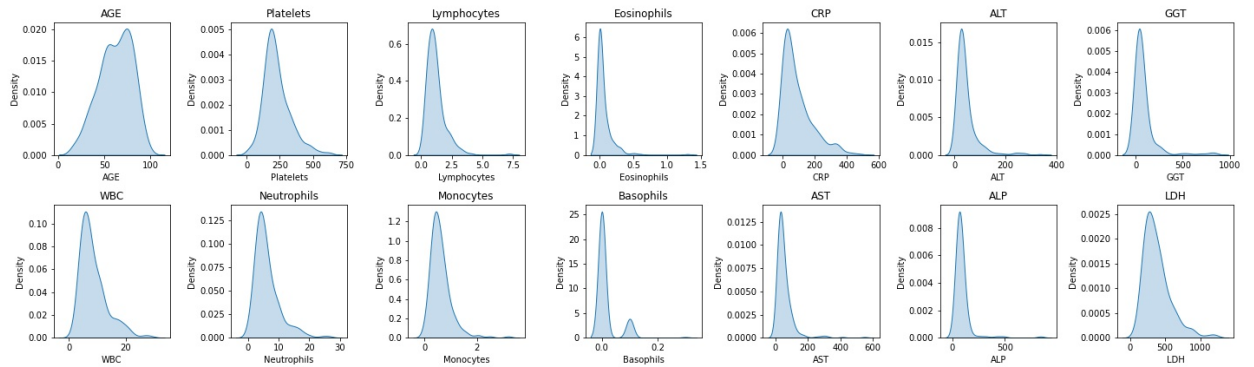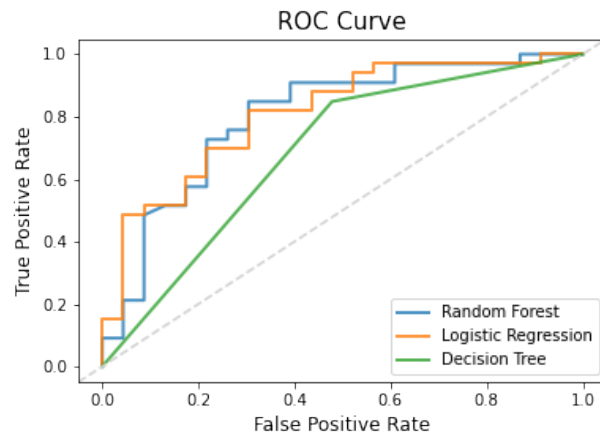
Appendix B

Supplementary Figures

Figure B.1: Kernel density plots of the numerical features of the data set
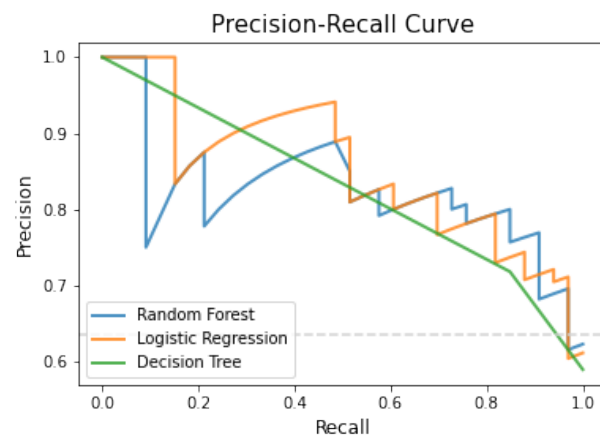

Figure B.2: K-fold nested cross validation [27]

(a) Receiver Operating Characterisitcs (ROC) curve

(b) Precision-Recall Curve

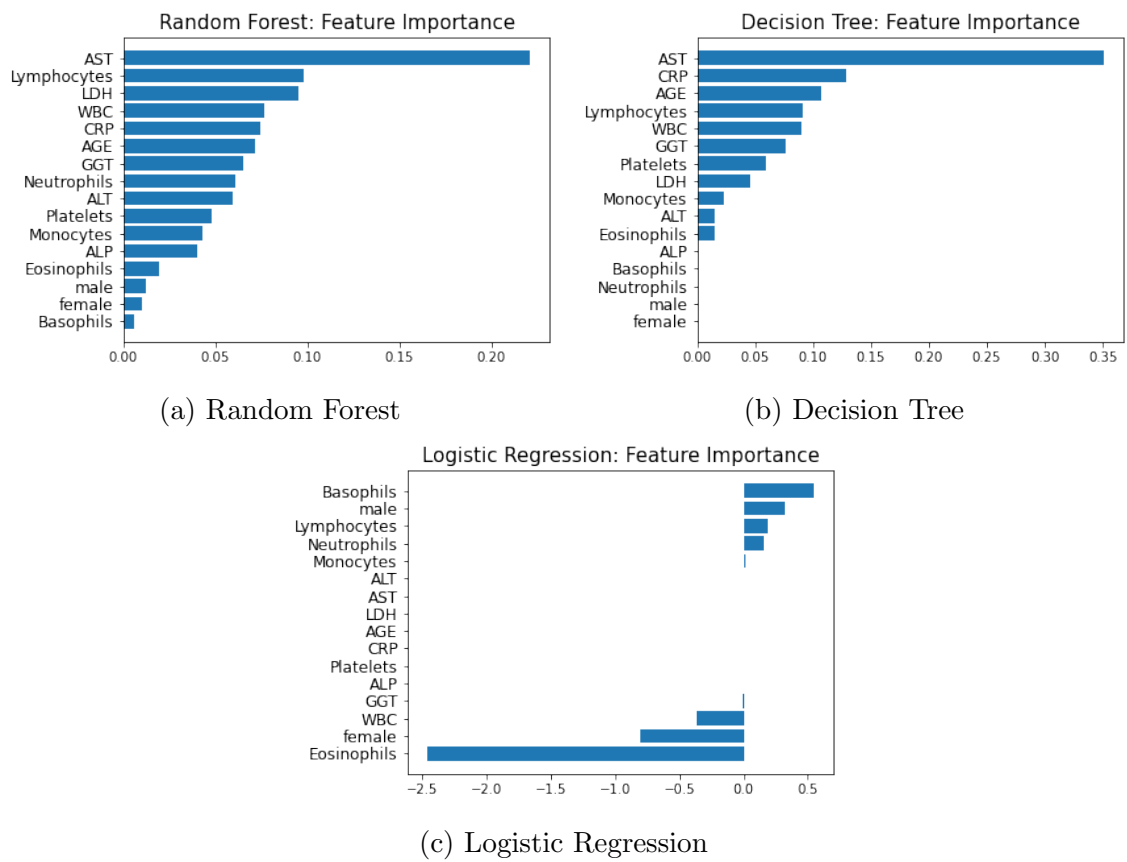Figure B.3: ROC and Precision-Recall curve

(a) Random Forest

(b) Decision Tree
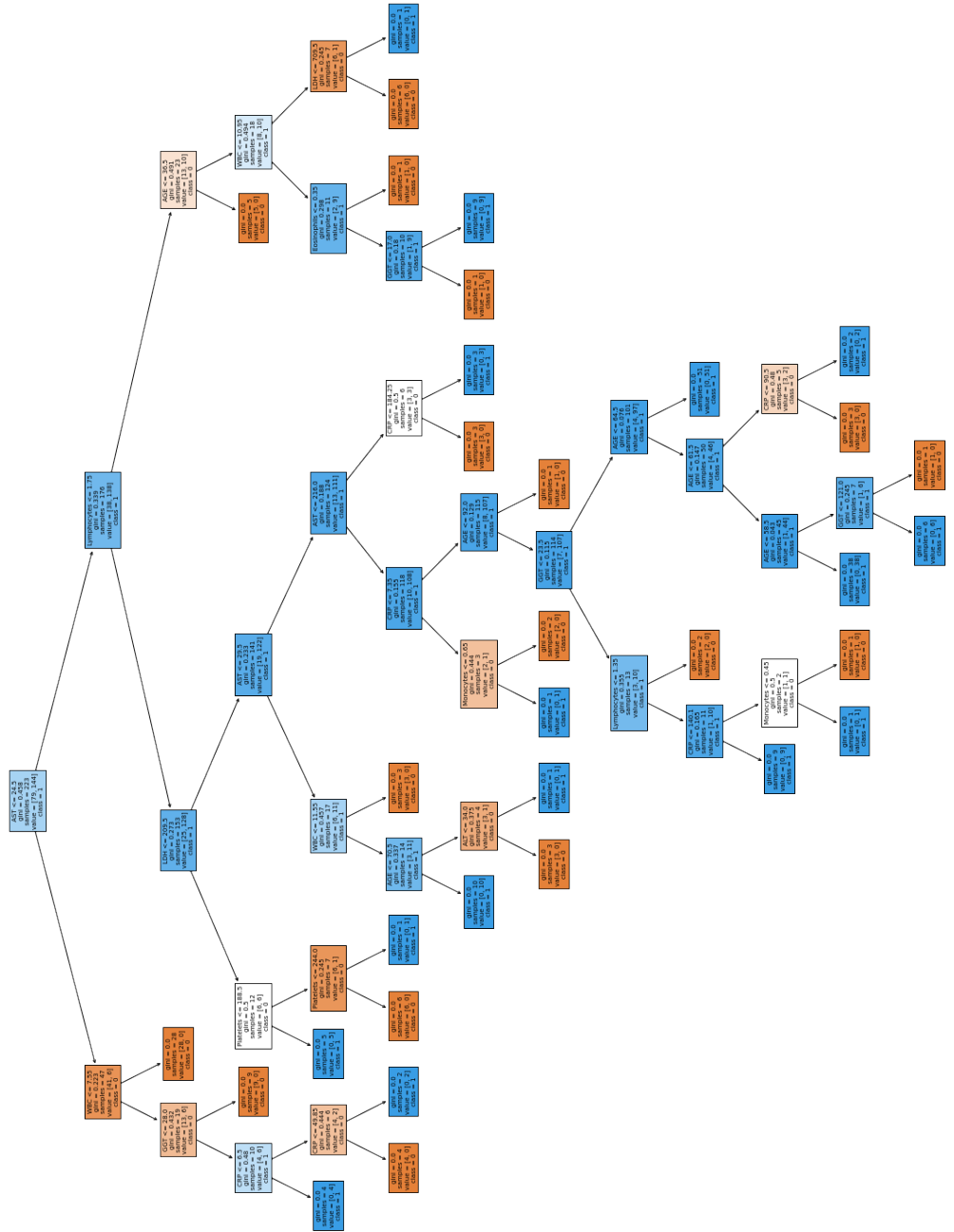
(c) Logistic Regression

Figure B.4: Feature importance plots

Figure B.5: Visualization of the Decision Tree produced during the validation phase

Appendix C

Supplementary Formulas

Bibliography

[1] A. K. Akobeng. "Understanding diagnostic tests 1: sensitivity, specificity and predictive values". In: *Acta Paediatr* 96.3 (2007), pp. 338–41. ISSN: 0803-5253 (Print) 0803-5253 (Linking). DOI: `10.1111/j.1651-2227.2006.00180.x`. URL: `https://www.ncbi.nlm.nih.gov/pubmed/17407452`.

[2] P. Allison. *Imputation by Predictive Mean Matching: Promise and Peril — Statistical Horizons.* 2015. URL: `https://statisticalhorizons.com/predictive-mean-matching`.

[3] *An Introduction to Statistical Learning.* Springer Texts in Statistics. 2013. ISBN: 978-1-4614-7137-0. DOI: `10.1007/978-1-4614-7138-7`.

[4] M. J. Azur et al. "Multiple imputation by chained equations: what is it and how does it work?" In: *Int J Methods Psychiatr Res* 20.1 (2011), pp. 40–9. ISSN: 1557-0657 (Electronic) 1049-8931 (Linking). DOI: `10.1002/mpr.329`. URL: `https://www.ncbi.nlm.nih.gov/pubmed/21499542,%20https://www.ncbi.nlm.nih.gov/pmc/articles/PMC3074241/pdf/MPR-20-40.pdf`.

[5] Leo Breiman. "Random Forests". In: *Machine Learning* 45.1 (2001), pp. 5–32. ISSN: 08856125. DOI: `10.1023/a:1010933404324`. URL: `https://link.springer.com/content/pdf/10.1023/A:1010933404324.pdf`.

[6] D. Brinati et al. "Detection of COVID-19 Infection from Routine Blood Exams with Machine Learning: A Feasibility Study". In: *J Med Syst* 44.8 (2020), p. 135. ISSN: 1573-689X (Electronic) 0148-5598 (Linking). DOI: `10.1007/s10916-020-01597-4`. URL: `https://www.ncbi.nlm.nih.gov/pubmed/32607737,%20https://www.ncbi.nlm.nih.gov/pmc/articles/PMC7326624/pdf/10916_2020_Article_1597%20.pdf,https://zenodo.org/record/3886927#.X3xhPO1CRPY`.

[7] Stef van Buuren. *Flexible Imputation of Missing Data, Second Edition.* 2nd ed. Boca Raton, Fla: CRC Press, 2018. ISBN: 978-0-429-96034-5. URL: `https://stefvanbuuren.name/fimd/`.

[8] Stef van Buuren and Karin Groothuis-Oudshoorn. "mice: Multivariate Imputation by Chained Equations inR". In: *Journal of Statistical Software* 45.3 (2011). ISSN: 1548-7660. DOI: `10.18637/jss.v045.i03`.

[9] F. Cabitza and J. D. Zeitoun. "The proof of the pudding: in praise of a culture of real-world validation for medical artificial intelligence". In: *Ann Transl Med* 7.8 (2019), p. 161. ISSN: 2305-5839 (Print) 2305-5839 (Linking). DOI: `10.21037/atm.2019.04.07`. URL: `https://www.ncbi.nlm.nih.gov/pubmed/31168442,%20https://www.ncbi.nlm.nih.gov/pmc/articles/PMC6526255/pdf/atm-07-08-161.pdf`.

[10] F. Cabitza et al. "Development, evaluation, and validation of machine learning models for COVID-19 detection based on routine blood tests". In: *Clin Chem Lab Med* (2020). ISSN: 1437-4331 (Electronic) 1434-6621 (Linking). DOI: `10.1515/cclm-2020-1294`. URL: `https://www.ncbi.nlm.nih.gov/pubmed/33079698,%20https://www.degruyter.com/downloadpdf/journals/cclm/ahead-of-print/article-10.15%2015-cclm-2020-1294/article-10.1515-cclm-2020-1294.pdf`.

[11] American Association for Clinical Chemistry. *Aspartate Aminotransferase (AST) — Lab Tests Online*. 2021. URL: `https://labtestsonline.org/tests/aspartate-aminotransferase-ast` (visited on 01/21/2021).

[12] American Association for Clinical Chemistry. *C-Reactive Protein - Understand the Test*. 2020. URL: `https://labtestsonline.org.uk/tests/c-reactive-protein`.

[13] American Association for Clinical Chemistry. *Full Blood Count - Understand the Test*. 2020. URL: `https://labtestsonline.org.uk/tests/full-blood-count-fbc` (visited on 10/25/2020).

[14] American Association for Clinical Chemistry. *Lactate Dehydrogenase (LDH) - Understand the Test*. 2021. URL: `https://labtestsonline.org/tests/lactate-dehydrogenase-ld` (visited on 01/21/2021).

[15] P. C. Chen, Y. Liu, and L. Peng. "How to develop machine learning models for healthcare". In: *Nat Mater* 18.5 (2019), pp. 410–414. ISSN: 1476-1122 (Print) 1476-1122 (Linking). DOI: `10.1038/s41563-019-0345-0`. URL: `https://www.ncbi.nlm.nih.gov/pubmed/31000806,%20https://www.nature.com/articles/s41563-019-0345-0.pdf`.

[16] M. P. Cheng et al. "Diagnostic Testing for Severe Acute Respiratory Syndrome-Related Coronavirus 2: A Narrative Review". In: *Ann Intern Med* 172.11 (2020), pp. 726–734. ISSN: 1539-3704 (Electronic) 0003-4819 (Linking). DOI: `10.7326/M20-1301`. URL: `https://www.ncbi.nlm.nih.gov/pubmed/`

32282894,%20https://www.ncbi.nlm.nih.gov/pmc/articles/PMC7170415/pdf/aim-olf-M201301.pdf.

[17] Jesse Davis and Mark Goadrich. "The relationship between Precision-Recall and ROC curves". In: *Journal* (2006), pp. 233–240. ISSN: ISSN. DOI: 10.1145/1143844.1143874. URL: https://dl.acm.org/doi/pdf/10.1145/1143844.1143874.

[18] D. K. Djakpo et al. "Blood routine test in mild and common 2019 coronavirus (COVID-19) patients". In: *Biosci Rep* 40.8 (2020). ISSN: 1573-4935 (Electronic) 0144-8463 (Linking). DOI: 10.1042/BSR20200817. URL: https://www.ncbi.nlm.nih.gov/pubmed/32725148,%20https://www.ncbi.nlm.nih.gov/pmc/articles/PMC7414516/pdf/bsr-40-bsr20200817.pdf.

[19] Ensheng Dong, Hongru Du, and Lauren Gardner. "An interactive web-based dashboard to track COVID-19 in real time". In: *The Lancet Infectious Diseases* 20.5 (2020), pp. 533–534. ISSN: 14733099. DOI: 10.1016/s1473-3099(20)30120-1.

[20] Tom Fawcett. "An introduction to ROC analysis". In: *Pattern Recognition Letters* 27.8 (2006), pp. 861–874. ISSN: 01678655. DOI: 10.1016/j.patrec.2005.10.010. URL: https://www.sciencedirect.com/science/article/abs/pii/S016786550500303X?via%3Dih%20ub.

[21] D. Ferrari et al. "Routine blood tests as a potential diagnostic tool for COVID-19". In: *Clin Chem Lab Med* 58.7 (2020), pp. 1095–1099. ISSN: 1437-4331 (Electronic) 1434-6621 (Linking). DOI: 10.1515/cclm-2020-0398. URL: https://www.ncbi.nlm.nih.gov/pubmed/32301746,%20https://www.degruyter.com/downloadpdf/journals/cclm/58/7/article-p1095.pdf.

[22] F. Gravetter and L. Wallnau. *Statistics for the behavioral sciences*. 9th ed. Belmont, CA: Wadsworth Cengage Learning, 2013. ISBN: 978-1-111-83099-1.

[23] Shachar Kaufman, Saharon Rosset, and Claudia Perlich. "Leakage in data mining". In: *Journal* (2011). ISSN: ISSN. DOI: 10.1145/2020408.2020496.

[24] John D. Kelleher, Aoife DArcy, and Brian Mac Namee. *Fundamentals of Machine Learning for Predictive Data Analytics: algorithms, worked examples, and case studies*. 1st ed. Camebridge, MA: The MIT Press, 2015. URL: https://mitpress.mit.edu/books/fundamentals-machine-learning-predictive-data-ana%20lytics.

[25] Gilles Louppe. "Understanding Random Forests: From Theory to Practice". Thesis. 2014. DOI: http://dx.doi.org/10.13140/2.1.1570.5928.

[26] G. Lu and J. Wang. "Dynamic changes in routine blood parameters of a severe COVID-19 case". In: *Clin Chim Acta* 508 (2020), pp. 98–102. ISSN: 1873-3492 (Electronic) 0009-8981 (Linking). DOI: 10.1016/j.cca.2020.04.034. URL: https://www.ncbi.nlm.nih.gov/pubmed/32405079,%20https://www.ncbi.nlm.nih.gov/pmc/articles/PMC7217800/pdf/main.pdf.

[27] A. J. Masino et al. "Machine learning models for early sepsis recognition in the neonatal intensive care unit using readily available electronic health record data". In: *PLoS One* 14.2 (2019), e0212665. ISSN: 1932-6203 (Electronic) 1932-6203 (Linking). DOI: 10.1371/journal.pone.0212665. URL: https://www.ncbi.nlm.nih.gov/pubmed/30794638.

[28] Christroph Molnar. *Interpretable Machine Learning*. Lulu.com, 2020. ISBN: 978-0-244-76852-2. URL: https://christophm.github.io/interpretable-ml-book/logistic.html.

[29] T. P. Morris, I. R. White, and P. Royston. "Tuning multiple imputation by predictive mean matching and local residual draws". In: *BMC Med Res Methodol* 14 (2014), p. 75. ISSN: 1471-2288 (Electronic) 1471-2288 (Linking). DOI: 10.1186/1471-2288-14-75. URL: https://www.ncbi.nlm.nih.gov/pubmed/24903709,%20https://www.ncbi.nlm.nih.gov/pmc/articles/PMC4051964/pdf/1471-2288-14-75.pdf.

[30] D. P. Oran and E. J. Topol. "Prevalence of Asymptomatic SARS-CoV-2 Infection : A Narrative Review". In: *Ann Intern Med* 173.5 (2020), pp. 362–367. ISSN: 1539-3704 (Electronic) 0003-4819 (Linking). DOI: 10.7326/M20-3012. URL: https://www.ncbi.nlm.nih.gov/pubmed/32491919.

[31] R. B. Parikh, Z. Obermeyer, and A. S. Navathe. "Regulation of predictive analytics in medicine". In: *Science* 363.6429 (2019), pp. 810–812. ISSN: 1095-9203 (Electronic) 0036-8075 (Linking). DOI: 10.1126/science.aaw0029. URL: https://www.ncbi.nlm.nih.gov/pubmed/30792287.

[32] F. Pedregosa et al. "Scikit-learn: Machine Learning in Python". In: *Journal of Machine Learning Research* 12 (2011), pp. 2825–2830.

[33] P. Poletti et al. "Age-specific SARS-CoV-2 infection fatality ratio and associated risk factors, Italy, February to April 2020". In: *Euro Surveill* 25.31 (2020). ISSN: 1560-7917 (Electronic) 1025-496X (Linking). DOI: 10.2807/1560-7917.ES.2020.25.31.2001383. URL: https://www.ncbi.nlm.nih.gov/pubmed/32762797,%20https://air.unimi.it/retrieve/handle/2434/763526/1557654/poletti%20eurosurv-25-3%201-1.pdf.

[34] J. R. Quinlan. "Induction of decision trees". In: *Machine Learning* 1.1 (1986), pp. 81–106. ISSN: 0885-6125 1573-0565. DOI: 10.1007/bf00116251. URL: https://link.springer.com/content/pdf/10.1007/BF00116251.pdf.

[35] Dagmar Reiche. *Roche Lexikon Medizin*. 5th ed. Munich: Elsevier Urban und Fischer, 2003. ISBN: 978-3-437-15156-9.

[36] L. Rokach and O. Maimon. "Top-Down Induction of Decision Trees Classifiers—A Survey". In: *IEEE Transactions on Systems, Man and Cybernetics, Part C (Applications and Reviews)* 35.4 (2005), pp. 476–487. ISSN: 1094-6977. DOI: 10.1109/tsmcc.2004.843247. URL: https://ieeexplore.ieee.org/document/1522531/.

[37] T. Saito and M. Rehmsmeier. "The precision-recall plot is more informative than the ROC plot when evaluating binary classifiers on imbalanced datasets". In: *PLoS One* 10.3 (2015), e0118432. ISSN: 1932-6203 (Electronic) 1932-6203 (Linking). DOI: 10.1371/journal.pone.0118432. URL: https://www.ncbi.nlm.nih.gov/pubmed/25738806,%20https://www.ncbi.nlm.nih.gov/pmc/articles/PMC4349800/pdf/pone.0118432.pdf.

[38] Shai Shalev-Shwartz and Shai Ben-David. *Understanding Machine Learning*. 2014. ISBN: 9781107298019. DOI: 10.1017/cbo9781107298019.

[39] S. S. Shapiro and M. B. Wilk. "An analysis of variance test for normality (complete samples)". In: *Biometrika* 52.3-4 (1965), pp. 591–611. ISSN: 0006-3444 1464-3510. DOI: 10.1093/biomet/52.3-4.591.

[40] S. Sun et al. "Abnormalities of peripheral blood system in patients with COVID-19 in Wenzhou, China". In: *Clin Chim Acta* 507 (2020), pp. 174–180. ISSN: 1873-3492 (Electronic) 0009-8981 (Linking). DOI: 10.1016/j.cca.2020.04.024. URL: https://www.ncbi.nlm.nih.gov/pubmed/32339487,%20https://www.ncbi.nlm.nih.gov/pmc/articles/PMC7194694/pdf/main.pdf.

[41] C. B. F. Vogels et al. "Analytical sensitivity and efficiency comparisons of SARS-CoV-2 RT-qPCR primer-probe sets". In: *Nat Microbiol* 5.10 (2020), pp. 1299–1305. ISSN: 2058-5276 (Electronic) 2058-5276 (Linking). DOI: 10.1038/s41564-020-0761-6. URL: https://www.ncbi.nlm.nih.gov/pubmed/32651556,%20https://www.nature.com/articles/s41564-020-0761-6.pdf.

[42] D. Wang et al. "Clinical Characteristics of 138 Hospitalized Patients With 2019 Novel Coronavirus-Infected Pneumonia in Wuhan, China". In: *JAMA* 323.11 (2020), pp. 1061–1069. ISSN: 1538-3598 (Electronic) 0098-7484 (Linking). DOI: 10.1001/jama.2020.1585. URL: https://www.ncbi.nlm.nih.gov/pubmed/

32031570 , %20https : // jamanetwork . com / journals / jama / articlepdf /
2761044/jama_wang_2020_oi_20001%209.pdf.

[43]   M. Weinstock et al. "Chest X-ray findings in 636 ambulatory patients with
       COVID-19 presenting to an urgent care center: a normal chest X-ray is no
       guarantee". In: *JUCM* 10 (2020), pp. 13–18. URL: https://www.jucm.com/
       documents/jucm-covid-19-studyepub-april-2020.pdf/.

[44]   I. R. White, P. Royston, and A. M. Wood. "Multiple imputation using chained
       equations: Issues and guidance for practice". In: *Stat Med* 30.4 (2011), pp. 377–
       99. ISSN: 1097-0258 (Electronic) 0277-6715 (Linking). DOI: 10.1002/sim.4067.
       URL: https : // www . ncbi . nlm . nih . gov / pubmed / 21225900 , %20https :
       //onlinelibrary.wiley.com/doi/abs/10.1002/sim.4067.

[45]   L. Wynants et al. "Prediction models for diagnosis and prognosis of covid-
       19 infection: systematic review and critical appraisal". In: *BMJ* 369 (2020),
       p. m1328. ISSN: 1756-1833 (Electronic) 0959-8138 (Linking). DOI: 10.1136/
       bmj.m1328. URL: https://www.ncbi.nlm.nih.gov/pubmed/32265220 ,
       %20https://www.bmj.com/content/bmj/369/bmj.m1328.full.pdf.